Journal of Sound and Vibration (2001) **247**(4), 683–702
doi:10.1006/jsvi.2001.3778, available online at http://www.idealibrary.com on IDEAL®

IMPROVED ESTIMATES FOR THE ENERGY CHARACTERISTICS OF A VIBRATING ELASTIC STRUCTURE VIA THE INPUT IMPEDANCE AND MOBILITY: EXPERIMENTAL VERIFICATION

YU. I. BOBROVNITSKII AND M. P. KOROTKOV

Laboratory of Structural Acoustics, Mechanical Engineering Research Institute of Russian Academy of Sciences, M. Kharitonievsky 4, 101990 *Moscow, Russian Federation. E-mail: bobrovni@orc.ru*

(*Received* 26 *May* 2000, *and in final form* 21 *April* 2001)

An efficient method for estimating the vibration energy characteristics (such as the potential energy, kinetic energy, loss factor, etc.) of a forced vibrating structure proposed earlier (*Journal of Sound and Vibration* 1998, **217**, 351–386) [1] is improved and validated numerically and experimentally. The main problem of experimental implementation of the method—differentiation of the measured input impedance and mobility with noise present—is solved with the help of the Padé approximation by ratios of polynomials. The results of computer simulation and laboratory experiment conducted on a flexurally vibrating beam show that the improved method gives reliable estimates of the vibration energy characteristics at low and middle frequencies.

1. INTRODUCTION

A very efficient method for estimating the energy characteristics of a linear elastic forced vibrating structure based on minimum measured data has been proposed in references [1, 2]. To obtain the potential energy, kinetic energy, loss factor, and other energy characteristics, one does not need, in this method, to measure or compute the vibration response over the entire structure; neither does one need to possess a vibrational model of the structure. The only quantities needed are the complex amplitudes of the external forces (or the input impedances of the structure with respect to these forces) and the complex amplitudes of velocity response at the driving points. In the simplest case, when the structure is driven by a single external force, it is sufficient to measure only two quantities: the amplitude of the force and amplitude of the driving point velocity. It was shown in references [1, 2] by computer simulation on simple structures (rod, plate) that the proposed method gave reliable estimates in the low and middle frequency range, but failed at certain natural frequencies of the structure. That was the main drawback of the method which excluded practical implementation.

One purpose of the present paper is to work out improved estimates that are free from this drawback. This is done in the form of correction coefficients for the estimates obtained in references [1, 2]. One other purpose of the paper is to describe experimental implementation of the method. The main problem here is in computing the derivatives with respect to frequency of the input impedance measured with noise: differentiation is known as an ill-conditioned operation unstable to input errors [3]. This problem is solved by using the so-called Padé approximation as a model of the measured input impedance.

0022-460X/01/440683 + 20 $35.00/0

A laboratory experiment has also been carried out to verify the method. The experimental results show that the energy characteristics obtained by the proposed method are in good agreement with those obtained by independent methods.

The structure of the paper is as follows. In section 2, improved estimates are derived. Results of the computer simulation demonstrating the accuracy of the improved estimates are presented in section 3. A laboratory experiment on a flexurally vibrating beam and its main results are described in section 4. The validity of the method is discussed in section 5. In section 6, the conclusion is drawn that the proposed economic method for estimating the energy characteristics of forced vibrating linear elastic structures is now well-based theoretically and sufficiently verified computationally and experimentally to be used practically.

2. CORRECTION COEFFICIENTS

2.1. BASIC RELATIONS

In this section, the basic relations of the method are recapitulated—see also references [1, 2]. Consider a finite linear elastic system with continuous or lumped parameters and with any type of damping, performing harmonic vibrations under the action of an external force $f \exp(-\mathrm{i}\omega t)$ concentrated at a point x_0 (other types of external loading are considered in reference [2]). Let the complex amplitude f of the force and the complex amplitude v of the driving point velocity response be known (or measured). The parameters of the system as well as the system response at other points are supposed unavailable. According to the proposed method [1, 2], one can, using the two available quantities, f and v, compute the *exact* values of the time-average vibration power dissipated in the system:

$$\mathbf{\Phi} = \frac{1}{2}|v|^2 \mathrm{Re}[z(\omega)] = \frac{1}{2}|f|^2 \mathrm{Re}[y(\omega)] \tag{1}$$

and the time-average Lagrange function L, i.e., difference between time-average kinetic energy T and potential energy U of the system:

$$L = T - U = -\frac{1}{4}|v|^2 \mathrm{Im}[z(\omega)/\omega] = -\frac{1}{4}|f|^2 \mathrm{Im}[y(\omega)/\omega]. \tag{2}$$

Here, the input impedance $z(\omega)$ and input mobility $y(\omega)$ are functions of the measured quantities:

$$z(\omega) = f/v, \quad y(\omega) = v/f. \tag{3}$$

Relations (1) and (2) are mathematically correct. If the input quantities, f and v, are known with absolute accuracy the dissipated power and Lagrange function may be computed with arbitrarily high accuracy.

All other vibration energy characteristics of the system may be expressed via the data, f and v, only approximately. The most important are the following approximate equations derived in references [1, 2] which relate the time-average total vibration energy E to the first derivatives with respect to frequency ω of the input impedance and mobility:

$$E = T + U \cong E_{imp} = -\frac{1}{4}|v|^2 \mathrm{Im}\left[\frac{\partial z(\omega)}{\partial \omega}\right], \tag{4}$$

$$E = T + U \cong E_{mob} = -\frac{1}{4}|f|^2 \operatorname{Im}\left[\frac{\partial y(\omega)}{\partial \omega}\right]. \tag{5}$$

The kinetic energy T, the potential energy U separately, the loss factor $\eta = \Phi/\omega E$, and the rest of the energy characteristics can be easily obtained as combinations of quantities (1)–(5). The basic approximate equations (4) and (5) determine the properties and accuracy of these combinations. Therefore, most attention is paid to the estimation of the total energy.

The main features of estimates (4) and (5), as established in references [1, 2], are the following. Estimate (4) of the total energy via the input impedance is very close to the exact values of E at all low and middle frequencies except in the vicinity of some antiresonance frequencies, while estimate (5) via the input mobility coincides with the exact values of E at all low and middle frequencies, but is erroneous in the vicinity of resonance frequencies of the system.

2.2. INPUT IMPEDANCE REPRESENTATION

The following representation of the input impedance will be used further,

$$z(\omega) = z_0 \frac{\Delta_r(\omega)}{\Delta_a(\omega)}, \tag{6}$$

where z_0 is a constant which is independent of frequency such as, for example, the characteristic impedance, $\Delta_r(\omega) = 0$ is the frequency equation of the system under study which is free of loading at the driving point x_0, and $\Delta_a(\omega) = 0$ is the frequency equation of the system with point x_0 fixed; subscripts r and a stand for resonance and antiresonance. Representation (6) can be derived from equations (3) as follows. When in the first equation (3), $f = z(\omega)v$, the loading f is zero, the vibration response v of the system may be non-zero only if impedance $z(\omega)$ is proportional to the function $\Delta_r(\omega)$. On the other hand, when in the second equation (3), $v = y(\omega)f$, the velocity amplitude at the point x_0 is zero, $v = 0$, that is to say, when the point x_0 is fixed, the system may vibrate non-trivially ($f \neq 0$) only if the mobility $y(\omega) = 1/z(\omega)$ is proportional to function $\Delta_a(\omega)$. Combining these two features leads to equation (6).

Representation (6) of the input impedance by the ratio of two functions of frequency, $\Delta_r(\omega)$ and $\Delta_a(\omega)$, is in fact very general and can be extended to any external loading. For example, if a linear system is driven by n point forces, it is characterized by a symmetric $n \times n$—matrix of the input impedances or $n \times n$—matrix of the input mobilities. In a similar manner as done above, it can be shown that each element of these matrices is proportional to the ratio of two functions of frequency corresponding to certain combinations of the free or fixed boundary conditions at n driving points. Examples of representation (6) of the input impedance with respect to a continuously distributed external load can be found, e.g., in reference [4].

For elastic systems described by linear differential equations and appropriate boundary conditions, functions $\Delta_r(\omega)$ and $\Delta_a(\omega)$ in representation (6) are entire functions of frequency. In particular, for discrete systems, e.g., for FE-models, they are polynomials and therefore can be expanded into finite products of linear functions, so that input impedance (6) can be represented as

$$z(\omega) = \mathrm{i}z_0 \frac{\prod_{n=1}^{N}(\omega - \Omega_{rn})}{\prod_{m=1}^{M}(\omega - \Omega_{am})}. \tag{7}$$

For systems with continuous parameters, the entire functions $\Delta_r(\omega)$ and $\Delta_a(\omega)$ are expanded into infinite products. However, in a bounded region of the complex plane ω, i.e., in a finite frequency range, they can be approximated by polynomials [5], and input impedance (6) thus can also be described by a rational function (7). Representations of type (7) are met in electric circuit theory [6] as well as in mechanics and acoustics [7]. In mathematics, the representation of functions by ratios of two polynomials is called the Padé approximation [8]. In section 4, it will be shown that the Padé approximation of the input impedance measured with random noise leads to minimum errors in estimating the energy characteristics.

The zeros of the numerators of equations (6) and (7), $\Omega_{rn} = \omega_{rn} - i\delta_{rn}$, are the complex eigenfrequencies of the system with zero load at point x_0. When the driving frequency is equal to one of them, $\omega = \omega_{rk}$, the input impedance is minimum and the response of the system at the point x_0 to the external force is maximum (resonance). The zeros of the denominators of equations (6) and (7), $\Omega_{am} = \omega_{am} - i\delta_{am}$, are complex eigenfrequencies of the system with the point x_0 fixed. At these frequencies, $\omega = \omega_{am}$, the input impedance is maximum, so that the response at the point x_0 to the external force is minimum (antiresonance).

2.3. CORRECTION COEFFICIENTS FOR E_{imp}

As mentioned in section 2.1, the estimate E_{imp} of the total energy via the input impedance given in equation (4) works well at low and middle frequencies but is erroneous near, and at, the antiresonance frequencies. In this section, a correction coefficient $\alpha(\omega)$ is derived which reconstructs the true values E of the total energy from the estimate E_{imp} in the vicinity of the antiresonance frequencies and does not change E_{imp} at other frequencies.

To illustrate the point, Figure 1 depicts the imaginary part of the input impedance and the ratio E_{imp}/E of estimate (4) to the exact value of the total energy (solid line in Figure 1(b)) for a system with two degrees of freedom (which is also studied in section 3.2). This system has one antiresonance frequency $\omega/\omega_1 = 2$, and therefore the ratio E_{imp}/E being equal to unity at all frequencies, differs from unity considerably in the vicinity of this frequency: at the frequency $\omega/\omega_1 = 2$ the ratio equals -1 (that means that the estimate E_{imp} is equal to the exact value of the energy with opposite sign) and at two frequencies—one to the left and another to the right of antiresonance frequency—the ratio and, hence, the estimate E_{imp}, is zero. It was directly verified that the curve E_{imp}/E in Figure 1(b) does not depend on the type of external excitation: it is the same for force excitation as well as for kinematic excitation. Thus, the ratio E_{imp}/E is a characteristic of the system and therefore, when specified independent of the exact value of the total energy, can be adopted as a correction coefficient for the energy estimate (4) via the input impedance. In other words, if a function of frequency, $\alpha(\omega)$, approximates closely enough to the ratio E_{imp}/E, then the quantity

$$\bar{E}_{imp} = E_{imp}/\alpha(\omega) \cong E \tag{8}$$

is the sought improved estimate for the total energy.

In what follows, such a correction function $\alpha(\omega)$ is obtained from characteristics of the input impedance, i.e., without using the exact value E. Let ω_1 and ω_2 be the frequencies at which the first derivative of the imaginary part of the input impedance with respect to frequency is zero (in Figure 1(a) these frequencies correspond to the minimum and maximum of the impedance curve). It can easily be verified that the function

$$\alpha(\omega) = \frac{(\omega - \omega_0)^2 - (\Delta\omega)^2}{(\omega - \omega_0)^2 + (\Delta\omega)^2} \tag{9}$$

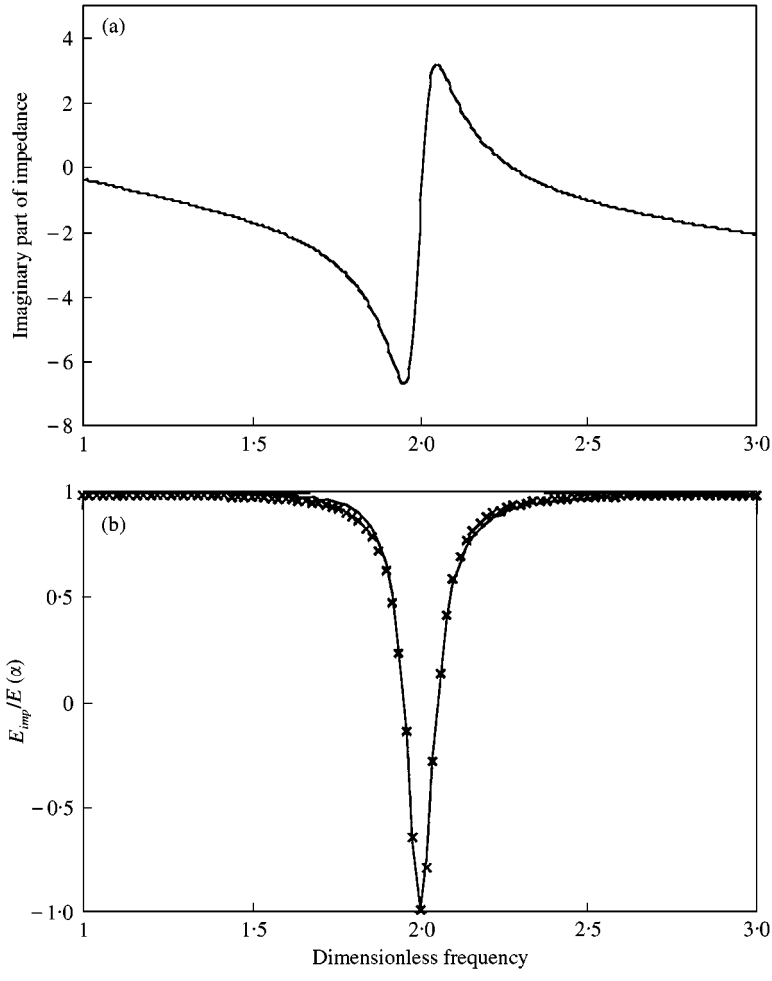

Figure 1. Imaginary part of the input impedance (a) and the estimate E_{imp} normalized by the exact value E of the total energy (——) and the correction coefficient α (× × × ×) (b) for the forced vibrating 2-d.o.f. system shown in Figure 2(b). Angular frequency ω is normalized by $\omega_1 = (k_1/m_1)^{1/2}$.

with $\omega_0 = (\omega_2 + \omega_1)/2$ and $\Delta\omega = (\omega_2 - \omega_1)/2$ has all the needed properties: it equals -1 at $\omega = \omega_0$, 0 at $\omega = \omega_1$ and ω_2, and $+1$ outside the vicinity of ω_0. This function is shown in Figure 1(b) by crosses. It is seen that it approximates the exact curve E_{imp}/E rather closely: the maximum deviation is smaller than 4·5%. Hence, within this accuracy, the improved estimate $\bar{E}_{imp}$ in equation (8), where $\alpha(\omega)$ is given in equation (9), equals the exact value of the total energy in the vicinity of the antiresonance frequency and does not degrade the estimate E_{imp} at other frequencies.

If the input impedance has several antiresonances, correction coefficient (9), $\alpha_k(\omega)$, may be computed for each antiresonance frequency ω_{ak} in the frequency range under study, the total correction coefficient $\alpha(\omega)$ being their product

$$\alpha(\omega) = \prod_k \alpha_k(\omega). \tag{10}$$

If a measured input impedance is represented as a Padé approximant (7), the correction coefficient $\alpha_k(\omega)$ may also be introduced directly into the derivative of the input impedance with respect to frequency,

$$\frac{\partial z(\omega)}{\partial \omega} = z(\omega)\left[\sum_n \frac{1}{\omega - \Omega_{rn}} - \sum_k \frac{(1/\alpha_k(\omega))}{\omega - \Omega_{ak}}\right], \tag{11}$$

before being substituted into equation (4) for estimating the total energy E. Note that for negative antiresonance frequencies, all $\alpha_k(\omega)$ in equation (11) should be equal to unity.

There are other functions that approximate the ratio E_{imp}/E and therefore may be used as correction coefficients. One such function is appropriate when the input impedance is available in the analytical form (6):

$$\alpha(\omega) \cong \frac{\operatorname{Re} \Delta_a^2}{|\Delta_a|^2}. \tag{12}$$

However, this function may have zeros at the frequencies that are slightly different from the roots of equation $E_{imp}(\omega) = 0$. Therefore, improved estimate (8) with coefficient (12) may (but not necessarily should) keep uncorrected the energy estimates in very narrow frequency bands ($\Delta\omega/\omega$ being of order of the squared system loss factor) near these root frequencies. Among possible functions, correction function (9) based on the exact roots of equation $E_{imp}(\omega) = 0$ is probably the best.

In computer simulation examples of section 3 and in the laboratory experiment of section 4 it will be shown that improved estimates (8)–(12) via the input impedance give good approximation to the total energy at each frequency of the low and middle frequency range, i.e., in the entire range of validity of the estimate E_{imp} itself.

2.4. CORRECTION COEFFICIENT FOR E_{mob}

Similar improved estimates of the total energy E, and hence of other energy characteristics, can be obtained starting from the second basic equation (5), i.e., from the estimate E_{mob} via the input mobility. This estimate should be corrected only near and at the resonance frequencies of a system. At other frequencies, including the antiresonance frequencies, the estimate E_{mob} is close enough to the true values of the total energy E and does not need any improvement.

As has been verified by the authors, the behaviour of the imaginary part of the input mobility in the vicinity of a resonance frequency is very similar to that of the imaginary part of the input impedance in the vicinity of an antiresonance frequency—see Figure 1(a). As a consequence, the ratio of estimate (5) to the exact value of the total energy, E_{mob}/E, is described by the same function of frequency as the ratio E_{imp}/E (shown in Figure 1(b)), the only difference being in replacing the antiresonance frequency by the resonance frequency. Therefore, the correction coefficient $\beta(\omega)$ for the estimate E_{mob} of the total energy via the input mobility is represented by the right-hand side of equation (9), the frequencies ω_1 and ω_2 being in this case the two roots of equation $E_{mob}(\omega) = 0$ in the vicinity of the corresponding resonance frequency. For such $\beta(\omega)$, the quantity

$$\bar{E}_{mob} \sim \frac{E_{mob}}{\beta(\omega)} \cong E \tag{13}$$

is the sought improved estimate.

For a measured mobility, represented as the Padé approximation, i.e., as a ratio of two polynomials of finite orders (see equation (7)), the correction coefficient $\beta_k(\omega)$ for each resonance frequency ω_{rk} should be introduced into the derivative of the input mobility:

$$\frac{\partial y(\omega)}{\partial \omega} = y(\omega)\left[\sum_n \frac{1}{\omega - \Omega_{an}} - \sum_k \frac{(1/\beta_k(\omega))}{\omega - \Omega_{rk}}\right]. \tag{14}$$

The substitution of this expression into equation (5) gives the correct estimates for the total energy in the entire frequency range under study.

3. COMPUTER SIMULATION EXAMPLES

To illustrate the accuracy of the improved estimates obtained, three simple mechanical systems are studied in this section—a single-degree-of-freedom-system (s.d.o.f.), a two-degree-of-freedom-system (2-d.o.f.), and, as an example of continuous structures, a longitudinally vibrating rod—see Figure 2.

3.1. s.d.o.f. SYSTEM

As the first example, consider a system with a single degree of freedom, consisting of a mass m, spring k and viscous damper c (Figure 2(a)). Its input impedance is equal to

$$z(\omega) = c + \mathrm{i}(k/\omega - m\omega) = z_0[\eta_0 + \mathrm{i}(\varepsilon^{-1} - \varepsilon)],$$

where $z_0 = m\omega_0 = \sqrt{mk}$ is the characteristic impedance, $\varepsilon = \omega/\omega_0$, $\omega_0 = \sqrt{k/m}$, and $\eta_0 = c/z_0$ is the loss factor of the system at the resonance frequency ω_0. It can be easily verified that unimproved estimate (4) via the input impedance gives here, i.e., for a system

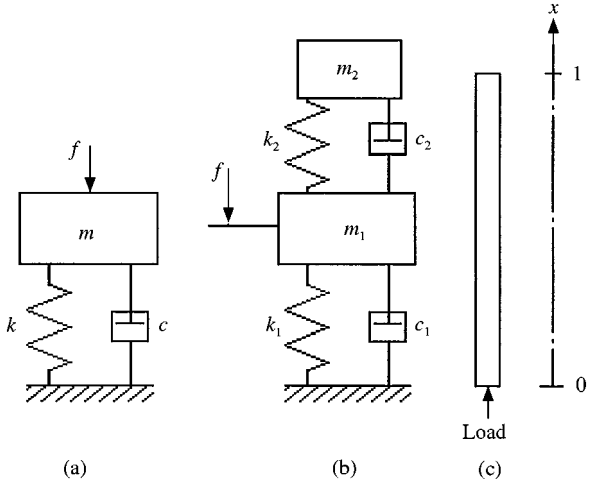

Figure 2. Forced vibrating mechanical systems studied in computer simulation: s.d.o.f. system (a), 2-d.o.f. system (b) and Bernoulli rod (c).

without antiresonances, the exact values of the total energy at all frequencies (u is the displacement amplitude):

$$E_{imp} = -\frac{1}{4}|v|^2 \operatorname{Im}\frac{\partial z(\omega)}{\partial \omega} = \frac{1}{4}k|u|^2 + \frac{1}{4}m|v|^2 = E.$$

Unimproved estimate (5) via the input mobility E_{mob}, also gives accurate values of the total energy everywhere except in the vicinity of the resonance frequency $\omega \cong \omega_0$. However, when improved estimate (13) with the correction coefficient (9) or (14) is used, the estimated values of E practically do not differ from the exact values. Figure 3 shows the loss factor of the s.d.o.f. system, computed from the equation

$$\eta(\omega) = \Phi/\omega E,$$

which is a general definition of the loss factor of a linear system vibrating at any frequency ω, with $\Phi = c|v|^2/2$ being the dissipated power. It is seen from Figure 3, that, when unimproved estimate (5) is used for computing the total energy, the loss factor is erroneous near $\omega = \omega_0$ (dotted line). However, when the improved equation is used, the estimate $\eta(\omega)$ is indiscernible from the true values of the loss factor (solid line).

3.2. 2-d.o.f. SYSTEM

Consider now a system with two degrees of freedom which has two resonances and one antiresonance—see Figure 2(b). The energy characteristics of this system, as well as their unimproved estimates via the input impedance and mobility have been studied in detail in reference [1]. Here, the effects of the correction coefficients on the estimates are demonstrated. The system input impedance at the first mass is

$$z(\omega) = -\mathrm{i}z_0 \Delta_r(\omega)/\Delta_a(\omega),$$

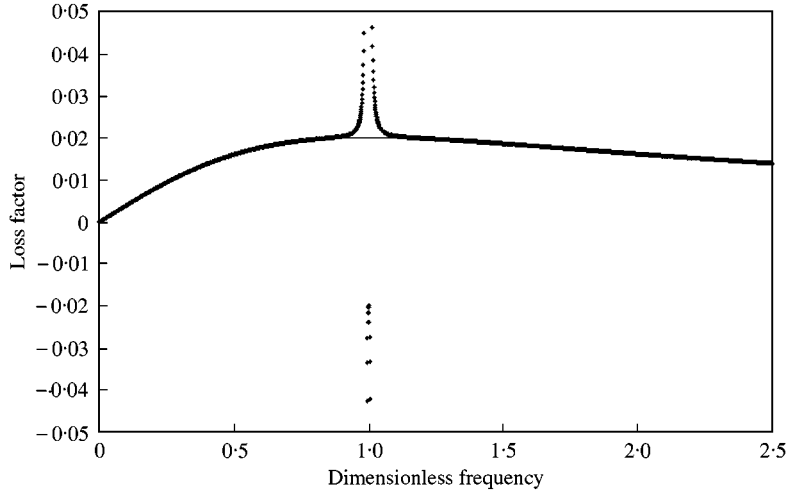

Figure 3. Loss factor of s.d.o.f. system (Figure 2(a)) as a function of frequency: the —— line represents the exact value and improved estimates (13), (14); the ··· line corresponds to unimproved estimate (5). Frequency is normalized by the resonance frequency $\omega_0 = \sqrt{k/m}$; the loss factor at $\omega = \omega_0$ is equal to $\eta_0 = 0{\cdot}02$.

where

$$\Delta_r(\omega) = [\omega^2 - (\omega_1^2 + \mu\omega_2^2) + \mathrm{i}\omega(\omega_1\eta_1 + \mu\omega_2\eta_2)](\omega^2 - \omega_2^2 + \mathrm{i}\omega\omega_2\eta_2) - \mu(\omega_2^2 - \mathrm{i}\omega\omega_2\eta_2)^2,$$

$$\Delta_a(\omega) = \omega\omega_1(\omega^2 - \omega_2^2 + \mathrm{i}\omega\omega_2\eta_2);$$

$$z_0 = \sqrt{m_1 k_1},\ \omega_1^2 = k_1/m_1,\ \omega_2^2 = k_2/m_2,\ \eta_1 = c_1/m_1\omega_1, \quad \eta_2 = c_2/m_2\omega_2, \quad \mu = m_2/m_1.$$

Antiresonance occurs here at the natural frequency of the subsystem $m_2/k_2/c_2$ which operates as a dynamic neutralizer with respect to the lower mass m_1.

Uncorrected estimate (4) of the system total energy via the input impedance works well at all frequencies except this antiresonance frequency—see dashed curves in Figure 4, the error being drastic in the case of kinematic excitation of the system where the response at the antiresonance frequency $\omega_a = 2\omega_1$ is dominant (Figure 4(b)). However, when estimate (8) is used together with correction coefficient (9), the estimated values of the total energy are practically identical to the exact values at all frequencies including the antiresonance one

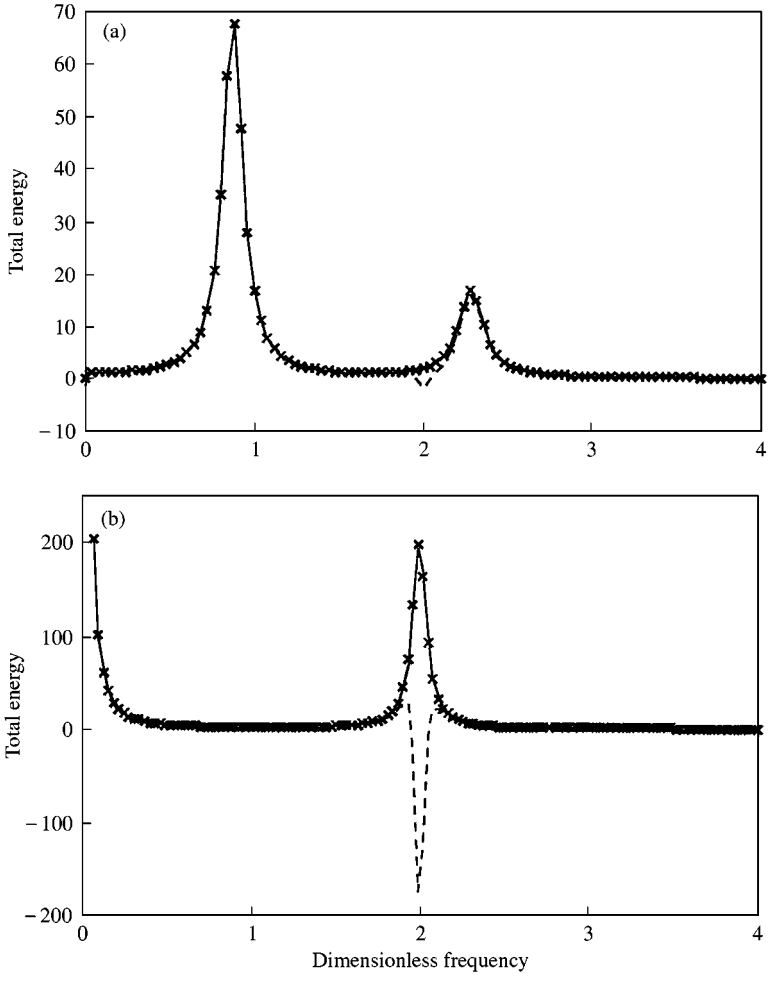

Figure 4. Normalized total energy of 2-d.o.f. system (Figure 2(b)) for force (a) and kinematic (b) excitation: exact (——), unimproved estimate (4) via impedance (– – – –) and improved estimate (8), (9) via impedance (× × × ×).

(crested lines in Figure 4). It is also seen from Figure 4 that corrected estimate (8) and (9) work well independent of the type of external excitation.

3.3. ROD

A straight uniform rod of a finite length l free of stress at one end executes longitudinal vibrations under the action of an external harmonic load applied to the other end - see Figure 2(c). The vibrations are assumed to be governed by the classical equation of Bernoulli with the complex Young's modulus, $E_c = E_0(1 - i\eta_0)$, η_0 being the material loss factor. The input impedance of the rod is equal to

$$z(\omega) = -iz_0 \frac{\sin kl}{\cos kl}, \tag{15}$$

where $z_0 = (E_c \rho S^2)^{1/2}$ is the characteristic impedance, ρ is the mass density, S is the cross-sectional area of the rod, $k = \omega(\rho/E_c)^{1/2} = k_0(1 - i\eta_0)^{-1/2}$ is the complex wavenumber, and $k_0 = \omega(\rho/E_0)^{1/2}$.

When the rod is excited kinematically, that is to say, when the vibration velocity amplitude at the driven end of the rod is kept equal to v_0 at all frequencies (never mind, what force is needed for that), the maximum response of the rod occurs at the antiresonance frequencies where input impedance (15) is maximum, $|\cos kl| = min$. This type of excitation is the worst for unimproved estimate (4) via the input impedance. However, when improved estimate (8) is used together with the correction coefficient (12)

$$\alpha(\omega) \cong \frac{\mathrm{Re}(\cos^2 kl)}{|\cos^2 kl|}, \tag{16}$$

the estimated values of the total energy are practically equal to the exact ones at low frequencies ($k_0 l < 8$) and do not differ from them by more than 10% at middle frequencies ($k_0 l < 20$)—see Figure 5. At higher frequencies ($k_0 l > 20$), the difference increases. The range of validity of the method itself is discussed in section 5.

Figure 6 shows the loss factor of the same rod excited this time by a force. As has been shown in references [1, 2], this energy characteristic is the most sensitive to the estimation errors in the total energy and, when unimproved estimate (4) is used, the loss factor can vary in a large range of magnitude. Figure 6 demonstrates that when improved estimates (8), (16) are used, the loss factor of the rod differs from the exact value no more than 6% in the range $k_0 l < 20$. The authors have also verified that when the rod is driven by a vibration source with an internal impedance, described in reference [1], the results of estimating the total energy and other energy characteristics are similar to those shown in Figure 5 or 6, independent of the value and type of the internal source impedance.

4. LABORATORY EXPERIMENT

To verify the proposed method of estimating the energy characteristics, a laboratory experiment on a flexurally vibrating beam has been carried out. Some results of the experiment that demonstrate the accuracy and efficiency of the method, as well as peculiarities of its practical implementation, are presented in this section.

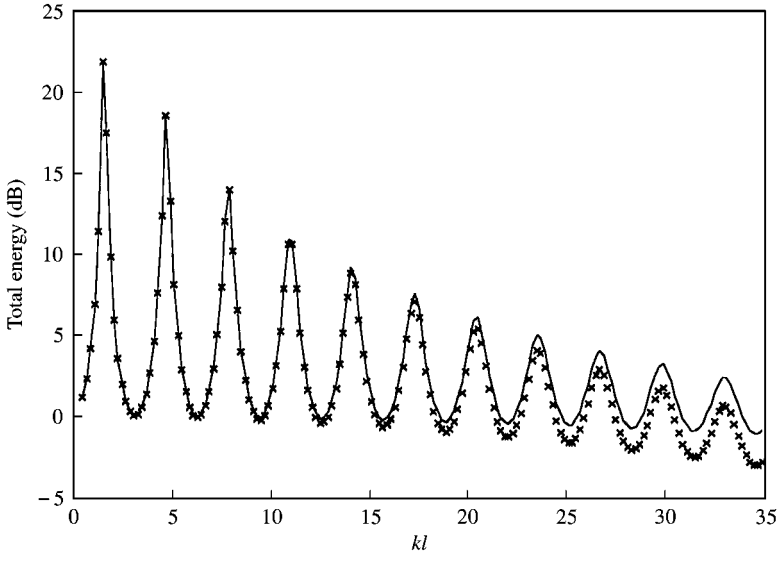

Figure 5. Total energy of a kinematically excited rod: exact (——) and improved estimate (8), (16) via the input impedance (× × × ×). Material loss factor is equal to 0·05.

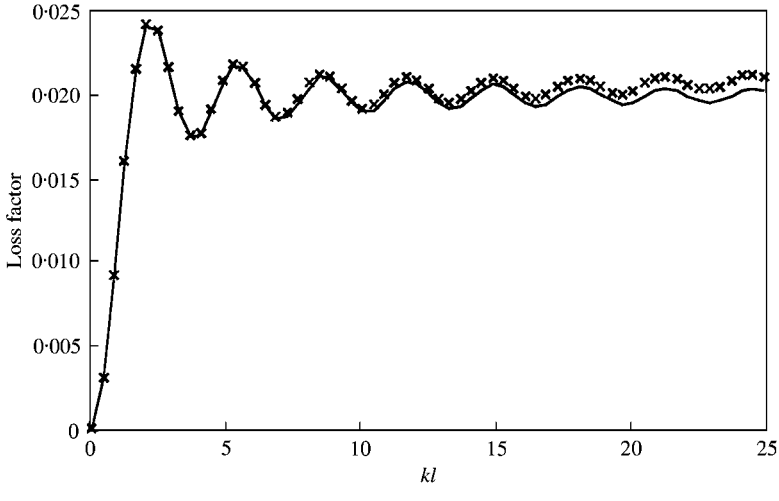

Figure 6. Loss factor of a forced vibrating rod: exact (——) and improved estimate (8), (16) via the input impedance (× × × ×). Material loss factor is 0·02.

4.1. EXPERIMENTAL SET-UP

The schematic of the experiment conducted is shown in Figure 7. A rectangular uniform beam of steel with dimensions in centimetres $4 \times 5 \times 150$, suspended on two wires, is driven harmonically in the horizontal plane by a shaker at one of its ends. The amplitudes and phases of the driving force $f(\omega)$ and acceleration $a(\omega)$ at the driving point (as well as at other points of the beam) are registered by a recorder as continuous functions of frequency and entered, at discrete frequencies, into a computer. As an example of these primary

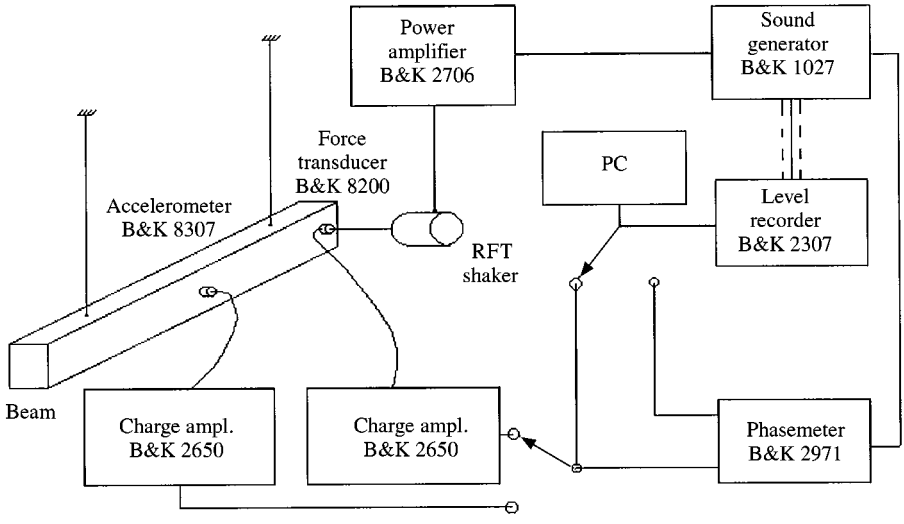

Figure 7. Experimental set-up.

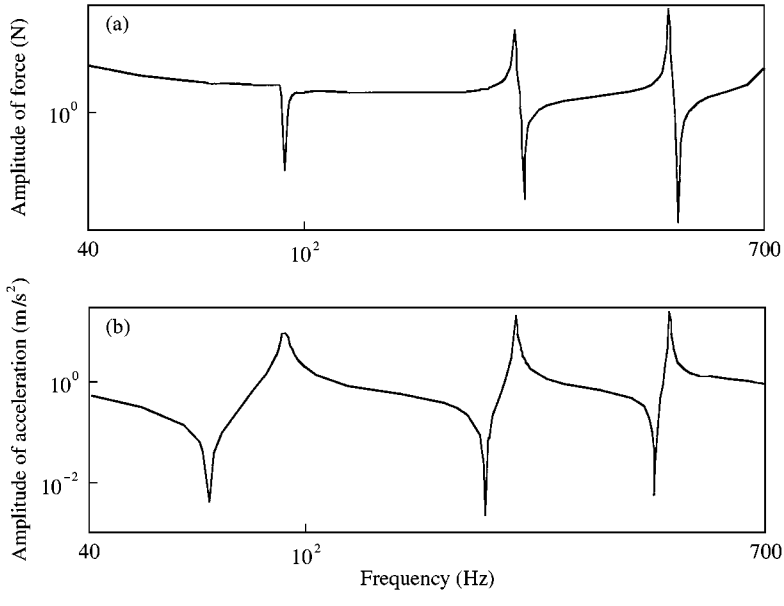

Figure 8. Measured amplitudes of external force (a) and driving point acceleration (b) for a flexurally vibrating beam.

experimental data, the measured amplitudes of the force and driving point acceleration are shown in Figure 8. One can see from the figure that the shaker used is not a source of constant amplitude force or of any kinematic quantity (acceleration, velocity, displacement). The force acting on the beam is constant only in some frequency regions, e.g., 100–200 Hz, while, at other frequencies, the amplitudes of the force and acceleration response vary within the range of 2–3 orders of magnitude.

Based on the measured functions $f(\omega)$ and $a(\omega)$, the velocity $v(\omega) = \mathrm{i}a(\omega)/\omega$, the input impedance $z(\omega) = f(\omega)/v(\omega)$, its reciprocal—the input mobility, their derivatives with respect to frequency, the energy estimates and all other necessary quantities in the experiment are obtained numerically in a computer.

4.2. DIFFERENTIATION PROBLEM

Figure 9 depicts by crosses the imaginary part of the measured input impedance or, more exactly, $\mathrm{Im}[z(\omega)]$ computed from the measured force and acceleration. As is seen from Figure 9, in the frequency range of measurement, 40–700 Hz, the beam has three resonance frequencies 92, 256 and 487 Hz, where the curve $\mathrm{Im}[z(\omega)]$ crosses the frequency axis, and three antiresonance frequencies 67, 214 and 439 Hz, where the curve rapidly varies from minimum to maximum. The quality factors of these resonances and antiresonances are rather high, $Q \cong 200$. Therefore, the rate of change of $\mathrm{Im}(z(\omega)]$ with frequency is also very high. For such data, which moreover are contaminated with noise, numerical computation of the derivatives with respect to frequency needed for the energy estimates becomes a problem. The authors have tried most of the available standard methods of numerical differentiation [9] but obtained rather poor results with large computation errors. One of the reasons for such errors is, of course, bad conditioning of the differentiation as a mathematical operation: small variations in a function can lead to large variations in its derivative [3]. However, the main reason here is that the standard methods are based on preliminary approximation (smoothing) of the data by polynomials which then are differentiated analytically. Functions like those shown in Figure 9 require high orders of the polynomials to be approximated with an acceptable accuracy. The orders of the polynomials used in the standard methods are actually insufficient for that purpose, especially, near the antiresonance frequencies where the impedance varies sharply.

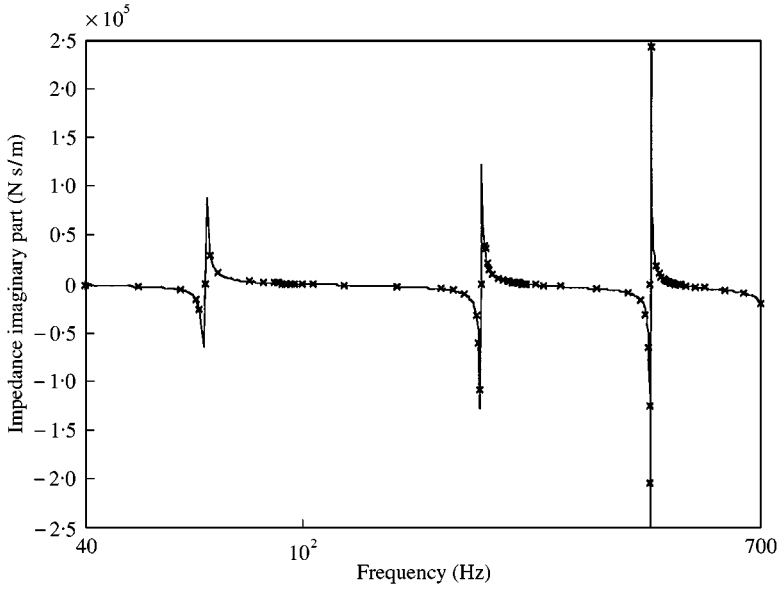

Figure 9. Imaginary part of the input impedance of a flexurally vibrating beam: measurements (× × × ×) and Padé approximant (——).

This differentiation problem has been overcome in the work with the help of the Padé approximation as a smoothing procedure for the input impedance and mobility. The Padé approximation, that is to say, the representation by a ratio of polynomials, follows, as was shown in section 2, from the general representation of the impedance by ratio of the entire functions and corresponds most closely to the spectral properties of a forced vibrating linear system (such as the interchange of resonance and antiresonance frequencies, a finite number of these frequencies in any bounded frequency range, etc.). The Padé approximation is, thus, a natural representation for the input impedances and mobilities and, therefore, even low order polynomials ratios may give good approximation. Namely, if the order of two polynomials is twice the number of resonance (antiresonance) frequencies in the frequency range under study, their ratio can provide very accurate approximation, not only to the input impedance and mobility, but to their derivatives as well.

4.3. PADÉ APPROXIMATION OF THE MEASURED INPUT IMPEDANCE

As the beam has, in the frequency range of interest, 40–700 Hz, four resonance frequencies (including $\omega = 0$) and three antiresonance frequencies, the approximant of Padé may be written as

$$z(\omega) = -\mathrm{i}\omega a \prod_{n=1}^{4} \frac{(\omega + \mathrm{i}\delta_{rn})^2 - \omega_{rn}^2}{(\omega + \mathrm{i}\delta_{an})^2 - \omega_{an}^2}. \tag{17}$$

It contains 17 unknown parameters—four complex resonance frequencies $\Omega_{rn} = \omega_{rn} - \mathrm{i}\delta_{rn}$, four complex antiresonance frequencies $\Omega_{an} = \omega_{an} - \mathrm{i}\delta_{an}$, and one real constant a responsible for the low-frequency behaviour of the impedance. All these parameters should be identified to match the experimental data. The following simple identification procedure is proposed and proved to be very efficient.

First, the real parts of the resonance frequencies, ω_{rn}, are determined. They correspond to minima of the experimental force amplitude curve (Figure 8(a)) and are equal to $\omega_{rn}/2\pi = 92$, 256, 487 and 795 Hz. Similarly, the real parts of the antiresonance frequencies are determined from the minima of the experimental acceleration amplitude curve in Figure 8(b), $\omega_{an}/2\pi = 67$, 214, 439 and 740 Hz. Note that the highest frequencies, ω_{r4} and ω_{a4}, lie outside the frequency range under study. They are included in the Padé model (17) for better approximation of the data at the upper end of the range, 600–700 Hz.

The next step is identification of the parameter a from the low-frequency values in Figure 9. The beam, being freely suspended, behaves at low frequencies as a mass, $z(\omega) \cong -\mathrm{i}\omega m_{eff}$. Upon assuming that, at low frequencies, the beam is near perfectly rigid, it can be shown from Newton's equations of mechanics that, with respect to the external force, its effective mass is $m_{eff} = M/4$, where $M = \rho Sl$ is the total mass of the beam ($M = 24$ kg for the beam used). The parameter a of model (17) is therefore equal to

$$a = \frac{M}{4} \prod_{1}^{4} \frac{\omega_{an}^2}{\omega_{rn}^2} = 9{\cdot}6 \text{ kg}.$$

Finally, eight damping coefficients δ_{rn} and δ_{an} are computed from the equality of the moduli of the experimental and modelling impedances at the resonance and antiresonance frequencies. Here, it was reasonably assumed that the impedance at each of these frequencies, say ω_{rk}, is determined only by the damping coefficient at this frequency, i.e., by δ_{rk}, so that all other coefficients, δ_{rn} and δ_{an} for $n \neq k$, may be set to zero. Thus, identified damping coefficients for the beam under study are: $\delta_{rn}/2\pi = 0{\cdot}09$, $0{\cdot}32$, $0{\cdot}28$ and $0{\cdot}35$ for

the resonance frequencies, and $\delta_{an}/2\pi = 0{\cdot}16$, $0{\cdot}09$, $0{\cdot}19$ and $0{\cdot}34$ for the antiresonance frequencies. For these values of the parameters, the mean square deviation of the experimental impedance is 1·2%. The solid line in Figure 9 corresponds to model (17). The agreement with the experiment (crosses) is excellent.

The authors also tried the Padé model of the type

$$z(\omega) = -\mathrm{i}\omega a \prod_{n=1}^{4} \frac{\omega - \omega_{rn} + \mathrm{i}\delta_{rn}}{\omega - \omega_{an} + \mathrm{i}\delta_{an}}, \tag{18}$$

which does not contain the negative eigenfrequencies and therefore is more simple than approximation (17). However, the accuracy of representation (18) is lower than that of approximation (17): the mean square deviation from the experimental data here is 7·6%.

4.4. ENERGY ESTIMATES

After the experimental impedance is approximated by rational function (17), its derivative with respect to frequency can be easily derived analytically in form (11) and further used for computing the improved estimates of the energy characteristics.

Such an obtained estimate of the total energy of the experimental beam is shown in Figure 10 by the solid line. The dashed line and the stars in Figure 10 correspond to the total energy obtained by two independent methods. As there do not exist methods for measuring directly the total energy of an elastic system, these two independent methods are based on computation of the energy in the classical flexural beam model of Bernoulli–Euler. The first method uses the analytical expression for the total energy and experimentally measured force amplitude and the beam loss factor (dashed line). In the second method,

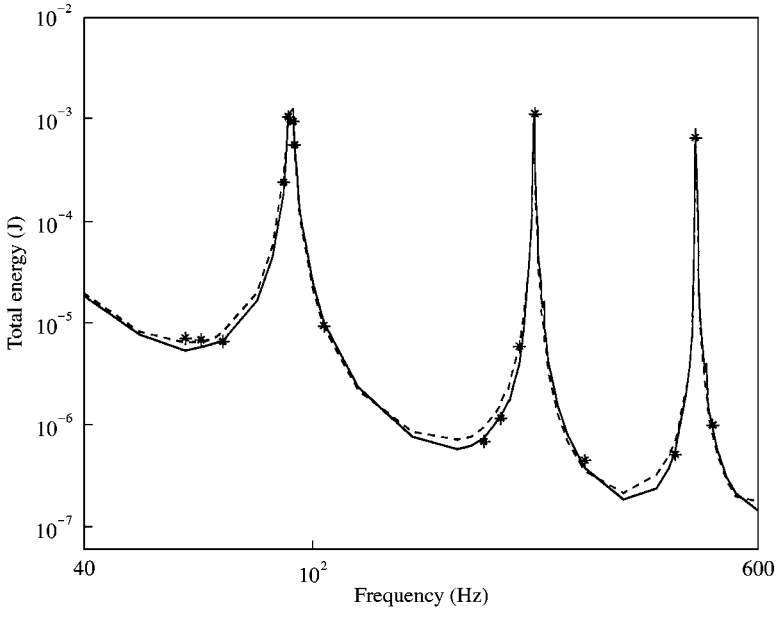

Figure 10. Total energy of the flexurally vibrating beam: measured by the proposed method (——) and by two independent methods (– – – – and ∗ ∗ ∗).

the total energy is computed from the distribution function of the vibration amplitude measured along the beam at several discrete frequencies (stars). As the beam in the frequency range under study is adequately described by the Bernoulli–Euler model, all such obtained values of the beam total energy were supposed to be close to its true values. More details about these two methods can be found in Appendix A.

It follows from Figure 10 that there is good agreement between the total energy values estimated by the improved method proposed in this paper and the values obtained by other methods. The experiment has, thus, confirmed that the proposed method gives reliable energy estimates at least at low and middle frequencies, where the measurements were made.

5. VALIDITY OF THE METHOD

As was pointed out above, the proposed method, when applied to not heavily damped structures, works well at low and middle frequencies, where the lengths of the elastic waves in the structure are greater than, or comparable with, its size. In this section, the frequency range of the method validity is discussed in more detail.

The external forces and the vibrational response at the driving points (or, equivalently, the input impedances (mobilities) and the velocity response) are the only quantities that are used in the method for estimating the energy characteristics of the entire structure. For the method to give the correct energy estimates, the response at the driving points should contain complete information about the vibrational behaviour of all parts of the structure or, in other words, the elastic waves reflected from all the structure boundaries should reach the driving points without noticeable attenuation due to damping. From this, it follows that the method is applicable only to finite structures which are not very much damped. It is proved in references [1, 2] that the method gives mathematically exact energy estimates for lossless finite linear structures. When it is applied to a damped continuous structure, the amount of information at the driving points may decrease and the method will give underestimated values of the structural energy. It is evident, for example, in Figure 5, that the estimated total energy of the rod as a function frequency is very similar to the exact function but its value is less than the exact one at all frequencies, the difference between them increasing with the structure length and frequency (damping is fixed). For this particular structure as well as for some other simple continuous structures (uniform beam, rectangular plate) of which the input impedance and any other quantities are available in an analytical form, the authors have found and verified that the decrease of the method accuracy can be approximately characterized by attenuation of the frequency response function (FRF) due to damping. More exactly, if $h(\eta_0, l)$ is the FRF of the structure (displacement or strain at one end when a load is applied to the other end), η_0 and l being the material loss factor and its dimension, the accuracy ac of the method defined as the energy ratio E_{imp}/E_{ex} (at resonance frequencies) is approximately described by the function $|h(\eta_0, l)/h(0, l)|^2$. It gives

$$ac(\eta_0, \omega, l) \cong \cosh^{-2}(\delta l) \tag{19a}$$

for one-dimensional structures (rods, beams), and

$$ac(\eta_0, \omega, l_1, l_2) \cong \cosh^{-2}(\delta l_1) \cosh^{-2}(\delta l_2) \tag{19b}$$

for two-dimensional structures ($l_1 \times l_2$-plates). Here, δ is the coefficient of spatial attenuation of the normal wave $\exp(\mathrm{i}kx - \mathrm{i}\omega t)$ in the structure: $\delta = \mathrm{Im}(k)$, k is the wavenumber. E.g., for the longitudinally vibrating rod one has

$$\delta = k_0 \mathrm{Im}(1 - \mathrm{i}\eta_0)^{-1/2} = \frac{\omega}{c_0} \sqrt{\frac{\sqrt{1 + \eta_0^2} - 1}{2(1 + \eta_0^2)}}$$

— see also equation (15). For flexurally vibrating beams and plates, the equation for δ is a little more complicated.

If a_0 is the required accuracy, then the inequality

$$ac \geqslant a_0 \tag{20}$$

with ac being function (19), approximately determines the range of validity of the method. For example, if the material loss factor of the rod studied above is equal to $\eta_0 = 0{\cdot}05$ the method provides the energy estimates with accuracy $a_0 = 0{\cdot}8$ (i.e., with the relative error $\leqslant 20\%$) up to the frequency $k_0 l = 25$, which corresponds to the eighth natural frequency of the rod. If the loss factor is $\eta_0 = 0{\cdot}01$, the frequency range of validity extends to the 40th natural frequency, etc. Inequality (20) can also be rewritten in terms of the rate of modal overlap. Then, for example, 20% error will be provided if the mode frequency band is less than one-third of the difference between adjacent eigenfrequencies.

It should be noted that, when the input impedance or mobility is available analytically, the exact values of all the energy characteristics can be reconstructed in any finite frequency range from the estimated values by means of the correction coefficients introduced above and by compensating the attenuation due to damping (19).

The correct values of the energy characteristics can also be reconstructed (and by this, the frequency range of the method validity can be increased) when some of the modal parameters of the structure are available. For example, if the input mobility of a rectangular simply supported $l_1 \times l_2$-plate is known in the form [1]

$$Y = A \sum_{m=1}^{M} \sum_{n=1}^{N} \frac{\gamma_{mn}}{\theta^4 - \theta_{mn}^4(1 - \mathrm{i}\eta_0)}, \tag{21}$$

where $\theta = kl_1$, is the dimensionless flexural wavenumber, $\theta_{mn}^2 = \pi(m^2 + n^2/b^2)$ is the (m, n)th resonance dimensionless frequency, $b = l_1/l_2$, the correct values of the plate total energy (and hence rest of the energy characteristics) can be obtained with the help of estimate (5) via the input mobility together with the correction coefficients

$$\beta_{mn} = \frac{(\theta^4 - \theta_{mn}^4)^2 - \eta_0^2 \theta_{mn}^8}{(\theta^4 - \theta_{mn}^4)^2 + \eta_0^2 \theta_{mn}^8} \tag{22}$$

introduced for each term of sum (21)—see also equation (14). The authors have verified that these improved estimates practically coincide with exact values in the frequency band where all the resonance frequencies θ_{mn}^2 are taken into account in equation (21). The reconstruction of the exact energy characteristics from the mobility estimates became possible in this case due to the additional information about global vibrational behaviour of the structure that the modal parameters, γ_{mn} and θ_{mn}, provide. Thus, if beside input impedance or mobility, some of the modal parameters (obtained, e.g., from FE-analysis) are available, the frequency range of the method validity can be expanded. In the limit, when the parameters of all N modes of a linear N d.o.f. system are known, the method gives the exact values of the energy characteristics at all frequencies.

Practically, the most important is the case when the input impedance or mobility is available from measurement, and nothing else is known about the structure under study. (This is just the case the proposed method has been developed for.) As follows from the results of section 4, to obtain the estimates in this case, one should first describe the measured impedance by Padé model (17) or (18) and identify its parameters, and then perform the necessary computations. The frequency range of the method validity is determined here by the accuracy of the Padé approximation or, more exactly, by the limitations of the parameter identification procedure used. The simplest procedure employed in section 4 is based on the assumption that the peaks of the vibration response (see Figure 8) are distinctly separated from each other, and the difference between two adjacent resonance frequencies is at least 3 times greater than the width of the resonance peaks. This comprises low and middle frequencies if the structure is not heavily damped ($\eta_0 < 0{\cdot}1$). So at present, it may be asserted that the proposed method works well just in this frequency range. However, the range can be increased if a more general procedure for identification of Padé model parameters is used. Such a procedure can be developed, most likely, by incorporating one of the advanced methods for parameter identification known in modal analysis [10, 11].

6. MAIN RESULTS AND CONCLUSION

The efficient method for estimating the energy characteristics of a linear forced vibrating structure, proposed earlier in references [1, 2], is improved in this paper: simple correction coefficients are derived that make the estimates accurate at low and middle frequencies. The improved method is validated by computer simulations and laboratory experiment. In the experimental implementation of this method, commercially available facilities and softwares (MATLAB) were used. The main implementation problem, the differentiation of noisy measured data, is solved by using the Padé approximation. From the results of this paper it can be concluded that the proposed method is theoretically based, validated sufficiently and now ready to be applied to the investigation of vibrations of practical structures.

At the same time, the method seems to have a great potential and therefore can be further improved. One of the possible improvements is its expansion to higher frequencies by using a more sophisticated procedure for the Padé model parameters identification.

ACKNOWLEDGMENT

The authors are greatly indebted to the referee for constructive comments and valuable suggestions.

REFERENCES

1. YU. I. BOBROVNITSKII 1998 *Journal of Sound and Vibration* **217**, 351–386. Estimating the vibration energy characteristics of an elastic structure via the input impedance and mobility. doi:10.1006/jsvi.1998.1806.
2. YU. I. BOBROVNITSKII 1999. *Acoustical Physics* **45**, 260–271. New method for estimating the energy characteristics of a vibrating elastic structure.
3. A. N. TIKHONOV and V. YA. ARSENIN 1977 *Solution of Ill-posed Problems*. Washington, DC: Simon & Schuster.

4. YU. I. BOBROVNITSKII and V. V. TYUTEKIN 1986 *Soviet Physics Acoustics* **32,** 408–413. Energy relations for compound waveguides.
5. B. YA. LEVIN 1956 *Root Distributions of Entire Functions*. Moscow: Nauka (in Russian).
6. S. KARNI 1996 *Network Theory: Analysis and Synthesis*. Boston, MA: Allyn and Bacon, Inc.
7. E. SKUDRZYK 1986 *Simple and Complex Vibratory Systems*. University Park: The Penn State University Press.
8. G. BAKER and P. GRAVE-MORRIS 1981 *Padé Approximante*. London: Addison-Wesley.
9. G. A. KORN and T. M. KORN 1961 *Mathematical Handbook for Scientists and Engineers*. NY: McGraw-Hill Book Company, Inc.
10. D. J. EWINS 1997 *Proceedings of the 6th International Conference on Recent Advances in Structural Dynamics, Southampton, U.K., Keynote Lecture*, 1–17. Recent advances in modal testing.
11. R. J. ALLEMANG and D. L. BROWN 1998 *Journal of Sound and Vibration* **211**, 301–332. A unified matrix polynomial approach to modal identification. Doi:10.1006/jsvi.1997.1321
12. K. F. GRAFF 1975 *Wave Motion in Elastic Solids*. Oxford: Clarendon Press.

APPENDIX A: TOTAL ENERGY OF THE BERNOULLI–EULER BEAM

Harmonic flexural vibrations of the classical one-dimensional model of Bernoulli–Euler are governed by the equation [12]

$$B\frac{\partial^4 w(x)}{\partial x^4} - \rho S\omega^2 w(x) = 0, \tag{A1}$$

where $w(x)$ is the displacement function, $B = E_c I$ is the flexural rigidity, ρ, l, S and I are the density, length, cross-sectional area and second moment, $E_c = E_0(1 - \mathrm{i}\eta_0)$ is the complex Young's modulus. The boundary conditions for the free beam driven by a force f at the end $x = l$ are

$$w''(0) = w'''(0) = 0, \quad w''(l) = 0, \quad Bw'''(l) = f \tag{A2}$$

with primes denoting the derivatives with respect to co-ordinate x. The solution to the boundary value problem (A1), (A2) is easily obtained as

$$w(x) = \frac{f}{(B/l^3)} \frac{(\mathrm{sh}\, kx - \sin kx)(\mathrm{ch}\, kl + \cos kl) - (\mathrm{ch}\, kx - \cos kx)(\mathrm{sh}\, kl + \sin kl)}{2(kl)^3(1 - \mathrm{ch}\, kl \cos kl)}. \tag{A3}$$

The input impedance of the beam is equal to

$$z(\omega) = f/(-\mathrm{i}\omega w(l)) = \mathrm{i}z_0 \Delta_r/\Delta_0,$$

where $k = (\rho S\omega^2/B)^{1/4}$ is the complex wave number, $z_0 = (\rho S l B/l^3)^{1/2}$ is the characteristic impedance; $\Delta_r = 1 - \mathrm{ch}\, kl \cos kl$ is the frequency equation of the free–free beam; $\Delta_a = \cos kl\, \mathrm{sh}\, kl/kl - \mathrm{ch}\, kl \sin kl/kl$ is the frequency equation of the beam free of traction at one end ($x = 0$) and hinged at the other end ($x = l$). When displacement function (A3) is found, the kinetic and potential energies of the beam, T and U, can be computed as

$$T = (1/4)\rho\, S\omega^2 \int_0^l |w(x)|^2\, \mathrm{d}x, \qquad U = (1/4)E_0\, I \int_0^l |w''(x)|^2\, \mathrm{d}x. \tag{A4}$$

In the laboratory experiment conducted in this work, it was first verified that the experimental beam, in the frequency range of interest, 40–700 Hz, was sufficiently accurately described by the Bernoulli–Euler model: it was found that the eigenfrequencies of the model computed from the roots of equations $\Delta_r = 0$ and $\Delta_a = 0$ deviated less than 2·5%

from the experimental resonance and antiresonance frequencies while deflection function (A3) was practically indiscernible from the displacement function measured at several arbitrary chosen frequencies. The loss factor of the model, η_0, which is unavailable *a priori*, was identified by the least-mean squares fitting acceleration response (A3) to the measured acceleration amplitudes at the resonance frequencies. The result is, $\eta_0 = 0{\cdot}004$.

The total energy of the beam flexural vibrations, $E = T + U$, was obtained, besides by the proposed method, by two different methods.

In the first method, it was computed by numerical integration of expressions (A4) with deflection function (A3) in which the force amplitude f and the material loss factor η_0 were taken from the experiment.

In the second method, the deflection function $w(x_j)$ was measured at 11 points along the beam, $j = 1, \ldots, 11$. Then, it was modelled by a linear combination of four flexural waves,

$$w(x) = a_1 e^{ikx} + a_2 e^{-ikx} + a_3 e^{-kx} + a_4 e^{-k(1-x)} \tag{A5}$$

and the model coefficients a_m were determined from the closeness of the measured data and equation (A5) in the least-mean squares sense. After that, function (A5) was substituted into equations (A4), the energy E computed.